Quench Detection for the Levitated Dipole Experiment (LDX) Charging Coil

Philip C. Michael, Darren T. Garnier, Alexi Radovinsky, Igor Rodin, Vladimir Ivkin, Michael E. Mauel, Valery Korsunsky, Sergey Egorov, Alex Zhukovsky, and Jay Kesner

***Abstract*—A NbTi charging coil (C-coil) for the Levitated Dipole Experiment (LDX) was manufactured by the Efremov Institute for the LDX team. The C-coil is used to inductively charge and discharge the persistent-mode, Nb_3Sn floating coil (F-coil) at the start and end of each series of plasma runs in the LDX. The intentional change of F-coil state has significant impact on the inductive voltage distribution within the C-coil during each charge/discharge cycle. Various techniques have been developed to facilitate quench detection in inductively coupled coils, the success of which depends on particularities of the application. This paper summarizes the evolution of the quench detection system applied to the LDX C-coil.**

***Index Terms*—Inductive coupling, magnet protection, quench detection.**

I. Introduction

THE Levitated Dipole Experiment (LDX) studies the behavior of high-beta plasmas confined by a dipole magnetic field. A ring-shaped Nb_3Sn coil (the F-coil) is electromagnetically supported near the center of a 5 m diameter by 3 m tall vacuum chamber to confine the plasma. The persistent-mode F-coil and cryostat with on-board helium supply operate without current leads or cryogenic connections through the plasma volume. The F-coil is inductively charged prior to a plasma run inside a large-bore NbTi coil (the C-coil).

Details of the C-coil design are presented in [1] and coupled operation of the C-coil and F-coil is presented in [2], [3]. The C-coil is a 1.3 m inner diameter, 0.75 m tall, layer-wound superconducting coil containing 48 layers and 8388 turns of NbTi superconductor cable. The C-coil has a self-inductance of 92.3 H and stores 8.3 MJ of magnetic energy at its rated operating current of 425 A. The C-coil is energized using a $\pm$40 V, $\pm$600 A, four-quadrant power supply, which limits its current change rate to within $\pm$0.4 A/s.

The C-coil design requirements specified peak hot spot temperature below 150 K following quench and peak discharge voltage via external dump resistor below 3 kV. To satisfy these requirements, the C-coil quench detection system must detect normal zone voltages by the time they reach 50 mV and then initiate within 100 ms the discharge of C-coil current through an external 5.7 Ω dump resistor. However, false detections, due to the change in C-coil inductive voltage distribution after the F-coil switches between normal and superconducting state, should be avoided. The quench protection system also discharges the C-coil current if the voltage drop along either vapor-cooled leads exceeds 100 mV.

Manuscript received August 29, 2006. This work was supported by the U.S. Department of Energy under Grant DE-EG02-98ER-54458/9.

P. C. Michael, A. Radovinsky, A. Zhukovsky, and J. Kesner are with the MIT-Plasma Science & Fusion Center, Cambridge, MA 02139 USA (e-mail: michael@psfc.mit.edu).

D. T. Garnier, and M. E. Mauel are with Columbia University, New York, NY USA.

I. Rodin, V. Ivkin, V. Korsunsky, and S. Egorov are with the Efremov Institute, St. Petersburg, Russia.

Digital Object Identifier 10.1109/TASC.2007.898071

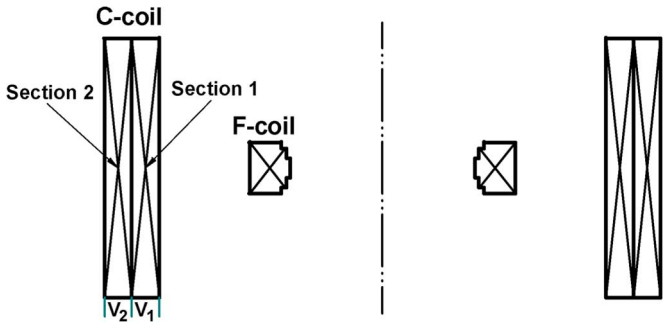

Fig. 1. Arrangement of the LDX C-coil and F-coil during inductive charging.

II. Balance Bridge Simulation

Use of a simple, three voltage tap balance-bridge for C-coil quench detection was simulated early during the coil design to illustrate the inadequacy of standard methods [4]. Fig. 1 shows the relative positions of the C-coil and F-coil during inductive charging. For this analysis, the C-coil is radially divided into two sections, with voltage V_1 across the inner section and voltage V_2 across the outer section. The quench detector balance voltage, $V_{qd} = f_n V_1 - V_2$, is computed throughout the charging cycle using a fixed balancing coefficient, f_n, that yields near zero offset voltage when the F-coil is in the normal state.

The equations used to model the approximately 60 minute inductive charging sequence are:

$$\begin{aligned} V_1 &= (L_1 + M_{12})\dot{I}_c + M_{1f}\dot{I}_f \\ V_2 &= (L_2 + M_{12})\dot{I}_c + M_{2f}\dot{I}_f \\ (M_{1f} + M_{2f})\dot{I}_c + L_f\dot{I}_f &= -(R_n + R_j)I_f : \mathrm{t} < 30 \\ (M_{1f} + M_{2f})\dot{I}_c + L_f\dot{I}_f &= -R_j I_f : \mathrm{t} > 30 \end{aligned} \quad (1)$$

Discharge of the F-coil current at the end of a plasma run is modeled similarly. L_1 and L_2 respectively are the self-inductances and M_{12} is the mutual inductance for the inner and outer sections for the C-coil. L_f is the self-inductance of the F-coil, while M_{1f} and M_{2f} respectively are the mutual inductances between the inner and outer sections of the C-coil and the F-coil. I_c is the C-coil current, while I_f is the F-coil current. R_n is the normal state resistivity of the F-coil at approximately 20 K

TABLE I
PARAMETERS FOR INDUCTIVE CHARGING SIMULATION

L_1	Self-inductance for C-coil section 1	28.61 H
M_{12}	Mutual inductance between C-coil sections 1 and 2	21.78 H
L_2	Self-inductance for C-coil section 2	20.12 H
L_f	F-coil self-inductance	0.399 H
M_{1f}	Mutual inductance, C-coil section 1 and F-coil	0.958 H
M_{2f}	Mutual inductance, C-coil section 2 and F-coil	0.711 H
R_n	F-coil normal state resistance (~20-K)	25.5 mΩ
R_j	F-coil close-out joint resistance	5 nΩ

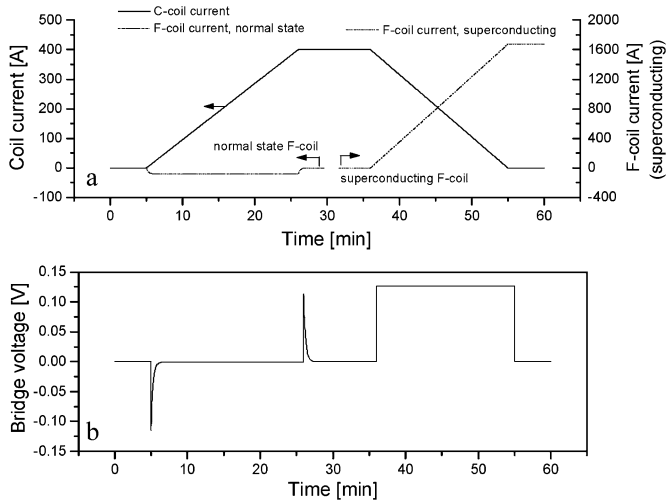

Fig. 2. (a) Variation in C-coil and F-coil currents, and (b) simulated bridge voltage during inductive charging simulation. Note that F-coil current axis changes from left-hand scale to right-hand scale during C-coil downramp.

and R_j is the resistance of the joint that short circuits the F-coil leads. Table I summarizes the simulation parameters, based on as-built coil dimensions. The bridge balance coefficient, f_n, is roughly equal to the ratio $(L_2 + M_{12})/(L_1 + M_{12})$, which is the exact solution with the F-coil removed from the system.

Fig. 2 shows results from the simulation. Fig. 2(a) shows the variation in C-coil and F-coil currents, while Fig. 2(b) shows the variation in balance bridge voltage. At the start of the simulation, the F-coil is a few degrees above its transition temperature. Starting 5 minutes into the simulation the C-coil current is ramped linearly to 400 A at 0.33 A/s. During the C-coil upramp about 20 A is induced in the normal state F-coil; at this value, the F-coil resistive voltage exactly balances the inductive voltage from the C-coil. The induced F-coil current decays rapidly at the end of the upramp.

While the C-coil current is held constant at 400 A, the F-coil temperature is reduced to 4.5 K by liquid helium transfer through an internal heat exchanger, and the F-coil becomes superconducting. Approximately 35 min into the simulation, the C-coil current is linearly ramped back to zero, inducing approximately 1.7 kA current in the F-coil.

The result in Fig. 2(b) shows that the C-coil requires a quench detector significantly more sophisticated than that provided by a simple balance bridge. The residual imbalance when current is induced in the F-coil is roughly 120 mV, which is more than twice the required normal zone detection sensitivity.

III. PROPOSED DIGITAL QUENCH DETECTOR

Fig. 3 shows a partial schematic of the quench detection system (QDS) developed by Efremov Institute for the C-coil

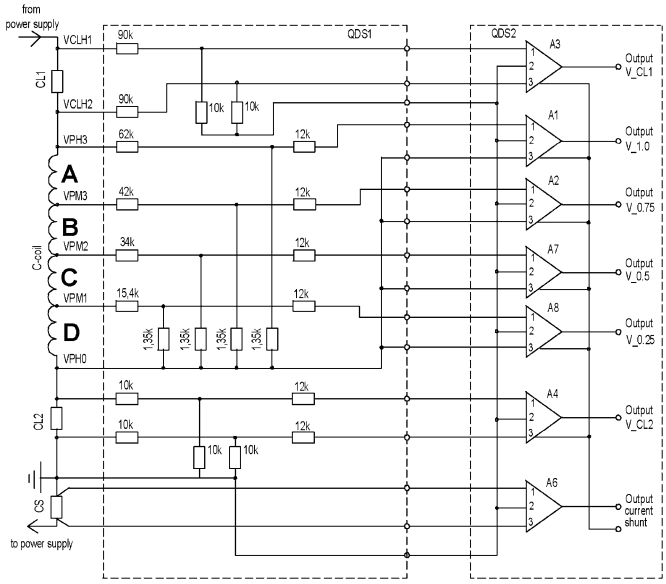

Fig. 3. Arrangement of the voltage divider designed for the C-coil.

[5]. The QDS is subdivided into two modules. QDS-1 contains a series of voltage dividers and QDS-2 contains a series of instrumentation amplifiers, a multiplexed 24 bit digitizer and a PIC16C877 microcontroller. Similar use of a microcontroller for magnet system monitoring is described in [6].

The C-coil power circuit is shown to the left-hand side of Fig. 3. A quench protection system (QPS), not shown in this figure, containing the dump resistor, is connected between the C-coil and its 6-pulse power supply. The high voltage side of the QPS is attached to the inner diameter of the C-coil through vapor cooled lead, CL-1. The C-coil is divided by voltage taps into four sections, labeled "A" through "D" in Fig. 3, starting from its inner diameter. Vapor cooled lead, CL-2, is grounded outside of the cryostat. A common ground is used for both power system and instrumentation. Shunt resistor, CS, measures the C-coil current. Neither F-coil current nor voltage is accessible for measurement.

The QDS-1 module contains two sets of voltage dividers. The first set was a pair of conventional balance bridges intended for stand-alone testing of the C-coil. The second set (shown in Fig. 3) scales the coil's nominal charging voltages, V_A through V_D, to the amplifiers' ± 1 V input range. The amplifiers are equipped with 4 Hz filters to suppress power supply noise. The amplifier outputs are also provided to the LDX programmable logic controller (PLC) for independent processing.

The design purpose for the second set of dividers was to facilitate implementation of a quench detection algorithm in the PIC microprocessor, based on the following equations:

$$V_{D1} = a_1 V_A + a_2 V_B + V_D$$
$$V_{D2} = b_1 V_A + b_2 V_C + V_D, \quad (2)$$

where V_{D1} and V_{D2} are digitally derived quench detection voltages, and a_1, a_2, b_1 and b_2 are the minimal numbers of coefficients theoretically needed to cancel all inductive voltages in the C-coil regardless of the state of the F-coil [7]. Two digital detection equations were used in (2) to facilitate redundant monitoring of the C-coil. A quench detection scheme similar to that in (2) was used to very good advantage for the superconducting

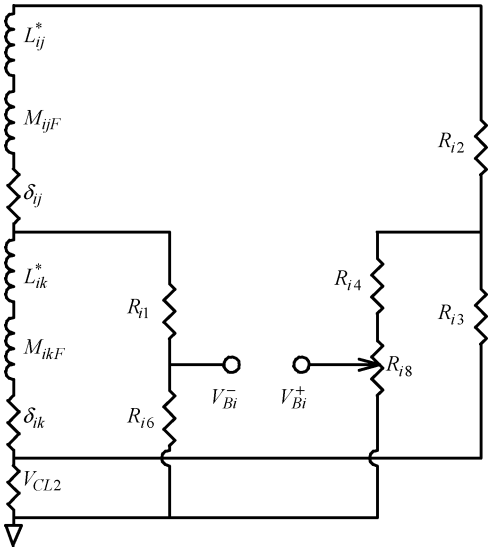

Fig. 4. Arrangement for the C-coil balance bridges.

outsert of the Francis Bitter National Magnet Laboratory's 30 T hybrid magnet [8].

The digital quench detection scheme developed for the C-coil was tried but never implemented for routine operation. Examination of signals recorded during coupled operation of the C-coil and F-coil reveals a small systematic error in the digitized coil voltages that yields large and variable offsets in the computed values of V_{D1} and V_{D2} to above the required detection threshold as the C-coil charging rate is changed [9]. As a result, an alternate quench detection scheme was developed using a combination of the conventional balance bridges in QDS-1, combined with expanded use of the facility PLC.

IV. Composite Quench Detection Scheme

The general arrangement of conventional balance bridges in the QDS-1 module is shown in Fig. 4. During development of the composite quench detection scheme an additional pair of balance bridges was installed, bringing the total to four. Of the four bridges, only three can be linearly independent, so there is some in-built redundancy in the scheme.

The subscript "i" in Fig. 4 refers to the bridge index number. The subscripts "j" and "k" are dummy variables that refer to the coil segments included in the bridge. For bridge 1, j corresponds to coil sections A and B, while k corresponds to sections C and D. For bridge 2, j corresponds to section C, while k corresponds to section D. For bridge 3, j corresponds to coil section B, while k corresponds to sections C and D. For bridge 4, j corresponds to coil section A, while k corresponds to sections B, C and D. The balance bridges retain the same instrument ground as in Fig. 3.

The output voltage from each balance bridge, V_{Bi}, is written:

$$V_{Bi}=f_i\alpha_i\left[V_{CL2}+\beta_i\left(\left(L^*_{ij}+L^*_{ik}\right)\dot{I}_c+(M_{ijF}+M_{ikF})\dot{I}_F +(\delta_{ij}+\delta_{ik})\right)\right]-\gamma_i\left[V_{CL2}+L^*_{ik}\dot{I}_c+M_{ikF}\dot{I}_F+\delta_{ik}\right] \quad (3)$$

where

$$\alpha_i=R_{i8}/(R_{i4}+R_{i8}),\quad \beta_i=R_{i3}/(R_{i2}+R_{i3}),$$
$$\gamma_i=R_{i6}/(R_{i1}+R_{i6}).$$

The effective self-inductances, L^*_{ij} and L^*_{ik}, in Fig. 4 are equal respectively to the self-inductance for that coil section plus the mutual inductance between that section and the rest of the C-coil. The mutual inductances between each coil section and the F-coil are represented by M_{ijF} and M_{ikF}. The normal zone voltages that are the object of the detection scheme are represented by δ_{ij} and δ_{ik}. V_{CL2} is the voltage along the vapor cooled lead attached to the coil ground. The resistor dividers, α_i, β_i and γ_i are used to limit the peak voltage to the QDS-2 amplifiers during high voltage dump of the C-coil current. Each bridge is balanced at low current (where the normal zone voltages δ_{ij} and δ_{ik} are assumed equal to zero) with the F-coil in the normal state, by adjusting the position, f_i, of trim pot R_{i8} in Fig. 4. When the bridges are balanced, $f_{i,bal}\approx\gamma_i L^*_{ik}/(\alpha_i\beta_i(L^*_{ij}+L^*_{ik}))$ and voltages due to inductive effects within the C-coil are eliminated. During subsequent C-coil current ramps with the F-coil in the superconducting state, the output from each balance bridge, $V_{Bi,bal}$, contains the following residuals:

$$V_{Bi,bal}=f_{i,bal}\alpha_i\beta_i(M_{ijF}\dot{I}_F+\delta_{ij}) +(f_{i,bal}\alpha_i\beta_i-\gamma_i)[V_{CL2}+M_{ikF}\dot{I}_F+\delta_{ik}] \quad (4)$$

The first step to implement the composite detection scheme is to numerically subtract in the PLC, the vapor-cooled lead voltages, V_{CL2}, from the bridge measurements. The measured bridge voltages, $V_{Bi,meas}$, (with V_{CL2} removed) are then scaled numerically to remove the effect of the voltage dividers, γ_i, and combined three at a time to form a set of four composite quench detection voltages, V_{Ci} [10]:

$$\begin{Bmatrix}V_{C1}\\V_{C2}\\V_{C3}\\V_{C4}\end{Bmatrix}=\begin{bmatrix}0.383 & 0.357 & -1 & 0\\ 0 & 0.425 & -1 & 0.404\\ -1 & 0 & 0.414 & 0.888\\ -0.947 & 0.166 & 0 & 1\end{bmatrix}\begin{Bmatrix}V_{B1,meas}/\gamma_1\\V_{B2,meas}/\gamma_2\\V_{B3,meas}/\gamma_3\\V_{B4,meas}/\gamma_4\end{Bmatrix} \quad (5)$$

Discharge of the C-coil current through the QPS is initiated whenever the absolute value for any one of the composite voltages exceeds 30 mV. The magnitudes of the measured bridge voltages are also monitored and compared against a typically higher detection threshold of 200 mV. By fortunate coincidence, the output from the second balance bridge, $V_{B2,meas}/\gamma_2$, is essentially free from inductive residuals (both in theory (4) and in practice) and a lower detection threshold of 25 mV is applied to this bridge.

The matrix used to generate the composite detection voltages in (5) is not unique and can vary depending on the objective function by which it is derived. Careful examination of balance bridge voltages during a dedicated series of moderate amplitude current ramps reveals the existence of inductive voltages in the C-coil that are not modeled in (3). For example, all balance bridges show significant offset during ramping below roughly 60 A, which we attribute to magnetization of cryostat and plasma vessel components. Thus, the C-coil quench detector is deactivated below 60 A, where risk and consequence of quenching is extremely low.

The composite detection matrix in (5) was derived to eliminate all residual inductive voltages from the balance bridge measurements, using data collected during C-coil current ramps

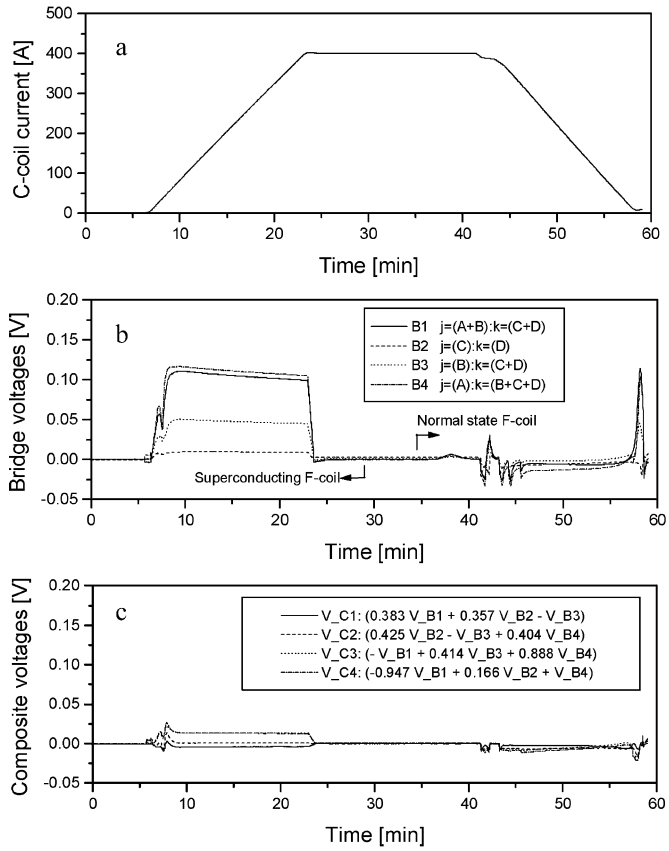

Fig. 5. (a) Time variation in C-coil current, (b) balance bridge voltages and (c) composite bridge voltages during inductive discharge of F-coil current.

with the F-coil in both normal and superconducting state [10]. For these matrix values, the composite quench detector activates for normal zone voltages of roughly 50 mV in C-coil sections B, C and D and 90 mV in section A. We are still reviewing the matrix values with the goal to increase the detection sensitivity for normal zones initiating in C-coil section A.

Fig. 5 shows the residual imbalance in bridge voltages, $V_{Bi,meas}/\gamma_1$, and composite voltages, V_{Ci}, during inductive discharge of F-coil current. Fig. 5(a) shows the time variation in C-coil current. Fig. 5(b) shows the bridge voltages and Fig. 5(c) shows the composite voltages. The residual imbalances in the composite voltages are sufficiently below the 30 mV quench detection threshold to permit reliable operation of the C-coil. Note that the inductive voltage spikes in the bridge voltages between 40 min and 45 min in Fig. 5(b), produced by non-steady control of the C-coil current down-ramp, are largely eliminated in the composite quench detection voltages in Fig. 5(c).

A quench detector roughly similar to composite scheme implemented for the C-coil was advocated by researchers at the University of Wisconsin (UW) several years ago [11]. However, this report was discovered only after the C-coil scheme had evolved to its present configuration.

V. Conclusion

A composite quench detection system, consisting of conventional balance bridges followed by digital processing, is an effective strategy for quench detection in the inductively coupled LDX C-coil. The residual imbalance in each C-coil balance bridge is typically less than 1/300 of the C-coil charging voltage. Inductive cancellation in the balance bridges significantly improves the accuracy of the digitized values needed for subsequent numerical processing. Empirical determination of the composite detection matrix was easy to accomplish. PLC processing permits additional control actions, such as the imposition of a 60 A current cut-off, below which the quench detector is deactivated. Logic programming also facilitates rapid reconfiguration of the detector by simply modifying a few lines of code; this feature was especially useful during initial tuning of the system.

LDX has been in routine operation since Aug. 2004. Since then, a single C-coil quench occurred due to a programming error in its current ramp generator. The quench was readily detected, with no ensuing damage to the C-coil.

References

[1] A. Zhukovsky, J. Schultz, B. Smith, A. Radovinsky, D. Garnier, and O. Filatov *et al.*, "Charging magnet for the floating coil of LDX," *IEEE Trans. Appl. Supercond.*, vol. 11, pp. 1873–1876, 2001.

[2] A. Zhukovsky, P. C. Michael, J. H. Schultz, B. A. Smith, J. V. Minervini, and J. Kesner *et al.*, "First integrated test of the superconducting magnet systems for the Levitated Dipole Experiment (LDX)," *Fus. Eng. Des.*, vol. 75–79, pp. 29–32, 2005.

[3] D. T. Garnier, A. K. Hansen, J. Kesner, M. E. Mauel, P. C. Michael, and J. V. Minervini *et al.*, "Design and initial operation of the LDX facility," *Fus. Eng. Des.*, 2006, in press.

[4] P. Michael, Simulation for coupled operation of the LDX C- and F-coils LDX project memo LDX-MIT-PCM-010121-01, MIT. Cambridge, Jan. 21, 2001.

[5] STC "SINTEZ" of the D. V. Efremov Scientific Research Institute, LDX Charging Coil—Quench Protection Unit of the Superconducting C-coil Efremov Document BI2-14-2003. St. Petersburg, July 1, 2003.

[6] O. O. Ige, D. Aized, D. Bushko, A. Curda, R. Medeiros, and G. Snitchler, "A demonstration HTS magnet for minesweeping application," *IEEE Trans. Appl. Supercond.*, vol. 10, pp. 482–485, 2000.

[7] A. Radovinsky and P. Michael, "C-Coil Quench Detection, Rev. 2," in *LDX Project Memo LDX-MIT-ARadovinsky-001003-01*. Cambridge: MIT, Oct. 3, 2000.

[8] T. Ishigohka and Y. Iwasa, "Protection of large superconducting magnets: A normal-zone voltage detection method," in *Proc. 10th Symp. Fus. Eng.*, 1983, pp. 2050–2053.

[9] D. Garnier, "D-mode QDS system analysis," in *LDX Project Memo LDX-CU-DTG-040129-01*. Cambridge: MIT, Jan. 29, 2004.

[10] D. T. Garnier, "LDX charging coil quench detection system: C+ mode," in *LDX Project Memo LDX-CU-DTG-050620-01*. Cambridge: MIT, June 20, 2005.

[11] M. A. Hilal, G. Vescey, J. M. Pfotenhauer, and F. Kessler, "Quench detection of multiple magnet system," *IEEE Trans. Appl. Supercond.*, vol. 4, pp. 109–114, 1994.